Evolutionary status and classification of selected neglected EBs observed with TESS

M. Vaňko

P. Gajdoš, M. Kamenec, R.Ch.R, Munagala, T. Pribulla, Š. Parimucha

Astronomical Institute, Slovak Academy of Sciences, Tatranská Lomnica
May 20, 2026

Outline

- Motivation
- The targets selection
- Light curves analysis
- Results and discussion
- The plans for future work

Motivation

- Avvakumova et al. (2013): Catalogue of Eclipsing Binaries.
- The study provided a comprehensive analysis of the distribution of observable stellar parameters for 7,179 eclipsing binaries (EBs) and developed an algorithm for their classification.
- In addition to the main catalogue (`catalog.dat`), the authors presented the following auxiliary lists of objects: `marginal.dat` and `lack.dat`.
- `marginal.dat`: The systems were found to belong to a 'marginal' (rare) type (93 objects). Some of these systems are in unusual stages of evolution. However, authors could not find an explanation for the peculiar values of the parameters for the majority of binaries listed there.
- `lack.dat`: The list contains systems with atypical (i.e. unreliable) parameter values and insufficient observations. There are 238 such systems in total.

Motivation (`marginal.dat`)

```
EK Cep    DM      Too large A1, far from line M for DM systems
EK Cep    DM      (see Fig.1 in Malkov et al. 2007, AA 465, 549).
EK Cep    DM      According to Popper [144] the radius and luminosity
EK Cep    DM      of the secondary components are enlarged in
EK Cep    DM      comparison with the MS star. Popper suggested the
EK Cep    DM      pre-MS status for this system.
EK Cep    DM      Later Marques et al. [260] have confirmed the pre-MS
EK Cep    DM      nature of the low mass secondary component of EK Cep.
BM Ori    DM      Possible pre-ms system
FF Aqr    DW      Period is significantly greater than typical value
FF Aqr    DW      for DW type. According to Pojmanski [45] this star
FF Aqr    DW      is DCEP-FU: variable. According to Sipahi et al. [263]
FF Aqr    DW      it is one of the few binary systems which consists of
FF Aqr    DW      the hot subdwarf and cool chromospherically active
FF Aqr    DW      giant components. According to Marilli et al. [264]
FF Aqr    DW      it is one of the peculiar system which is defined as
FF Aqr    DW      pre-cataclysmic binaries or pre-symbiotics.
RR Cae    DW      Pre-cataclysmic system (see Bruch
RR Cae    DW      [1999AJ....117.3031B]), A1 is greater than 3.
RR Cae    DW      Post-common-envelope binary according to
RR Cae    DW      Parsons et al. [2010arXiv1005.3958P].
UU Sge    DW      Too large A2 and A1 is greater than 3, lies far from
UU Sge    DW      other DW systems. UU Sge is the nucleus of planetary
UU Sge    DW      nebula Abell 63 and thus post-CE binary. According to
UU Sge    DW      Afsar & Ibanoglu [261] radius and temperature of the
UU Sge    DW      secondary component are larger than those expected
UU Sge    DW      for MS star of the same mass. Derived limb darkening
UU Sge    DW      coefficients of the secondary corresponds to a
UU Sge    DW      temperature about 10000K. Perhaps the large value of
UU Sge    DW      A2 is due the reflection effect and overheated face
UU Sge    DW      of the secondary.
BE UMa    DW      Period is greater than 1d. Young pre-cataclysmic
BE UMa    DW      variable (Shimanskii et al. [197]). Strong reflection
```

Motivation (`lack.dat`)

```
XZ And    SA      DI!=DII, without confirmation
CD And            System can belong to DGlate only because of its
CD And            large period, but A2 is not suitable for DG.
CD And            According to Kreiner [1] period = 34.4434. And then
CD And            it is not DG, but DM or SA. Only old photographic
CD And            data are available. So confirmation of value of the
CD And            period and new observations are necessary.
V374 And          To classify as DM new value of A1 is necessary.
V374 And          Semi-regular pulsating star in Simbad. Is system
V374 And          really eclipsing?
V395 And  C       May belong to CE only but spectra is somewhat later
V395 And  C       than needed
V413 And          Period is large to classify as SA, period is short
V413 And          to classify as DGlate. There is no individual
V413 And          investigations.
AP Aps            Only photographic data are known, value of A2 is
AP Aps            large. EB light curve with two equal minima.
AP Aps            Period may be twice shorter? More observations and
AP Aps            investigation are needed.
BQ Aqr            System may belong to SA class, but secondary spectra
BQ Aqr            must be measured.
KV Aqr            System will belong to D2S or SA if curve type
KV Aqr            (EA or EB) is given.
Y Aql             System can be classified, if luminosity class will
Y Aql             be determined properly.
V413 Aql          System may be classified as DGlate or D2S, if
V413 Aql          spectra will be determined properly.
V719 Aql          Value of A1 is large, old photographic data only.
V885 Aql          New photometry is required to classify this system
V885 Aql          as DM or SH.
V1251 Aql         Old photographic data only, period =1d is not
V1251 Aql         suitable for ASAS-3 light curve.
```

Target selection

- Focusing on systems: (i) No individual investigations have been conducted to date.
  (ii) Binaries that have not been studied in greater depth.
- For an eclipsing binary to be included, an additional criterion is that its orbital period must be shorter than 27 days, which corresponds to the length of the TESS satellite's photometric runs.
- We have identified (or pre-selected) 253 candidates that could be suitable for further processing.
- We retrieved all available data for these objects from the TESS satellite, prioritising unprocessed full-frame image (FFI) data.
- We performed detrending using custom Python-based tools built on the `Lightkurve` package (Lightkurve Collaboration, 2018). Background subtraction and flattening were then applied to the raw data to remove unwanted trends and artefacts.
- Phase curves were constructed from the resulting light curves (LCs). A narrower subset of objects was then selected for further analysis based on these curves.

Target selection

- The second step of the process involved the following selection criteria:

  (i) We excluded objects with periods exceeding 15 days. This limit was chosen primarily because TESS observes a given sector for around 27 days, so obtaining as many cycles as possible for each object was necessary.

  (ii) Also, objects with insufficient data coverage (e.g. only one or two sectors) and poor data quality (e.g. caused by instrumental effects, contamination from external light sources, thermal variations and, for fainter objects, shot noise) were excluded.

  (iii) We did not consider a group of misclassified objects (e.g. pulsating variables) or systems that were unsuitable for our study for various reasons (e.g. significant non-periodic irregularities in the light curves or the presence of Wolf-Rayet stars).

- A final sample of 102 eclipsing variables was selected for photometric analysis. These included *detached*, *semi-detached* and *over-contact* systems, for which the presence of starspots and other secondary effects was anticipated.

- In addition, we identified a group of 14 objects that could not be analysed in this paper due to time constraints. The analysis of their light curves requires a more in-depth study of the effects involved.

Target selection

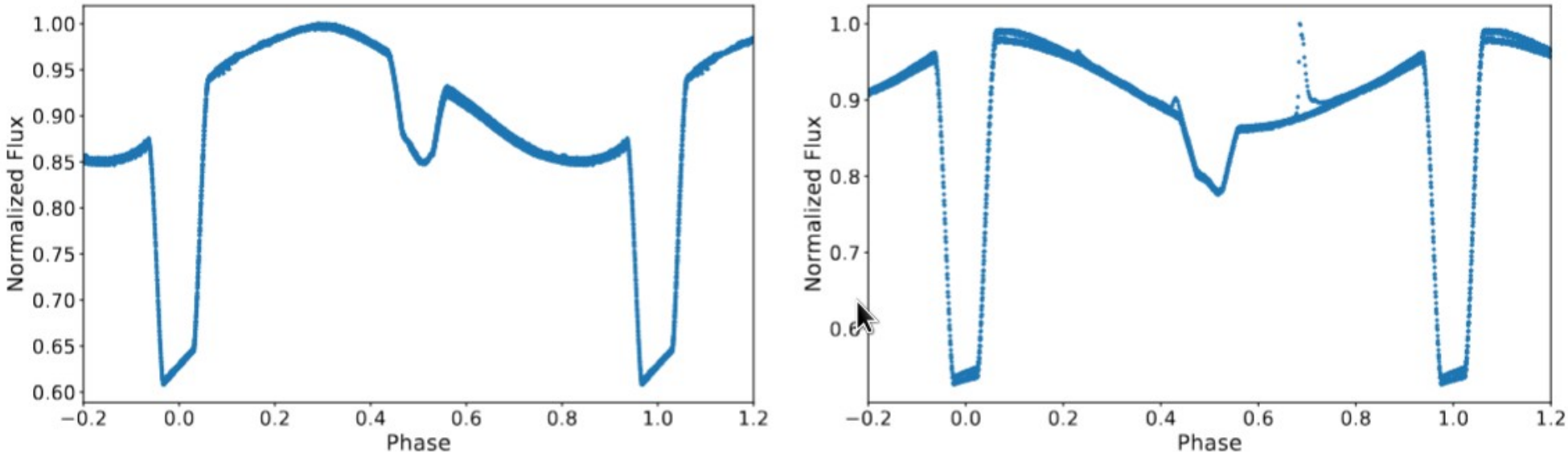

Figure 1. Light curves of BQ Aqr (*left*) and TU Cet (*right*) as an example of systems with unusual features on LC. Both systems are, very probably, spotted binaries. In the case of TU Cet a flare is clearly visible around photometric phase 0.7.

Target selection

Table 1. Description for selected targets.

Object	α_{2000}	δ_{2000}	$V_{\max}$ [mag]	$J-K$ [mag]	π [mas]	$T_{\rm eff}$ [K]	Class.
XZ And	01 56 51.5	+42 06 02	9.91	0.185(35)	1.933(59)	–	EA
V0395 And	23 44 32.1	+46 22 48	7.55	-0.116(25)	2.340(29)	12622^{+100}_{-50}	EW
BQ Aqr	23 36 09.0	-16 28 08	10.07	0.712(37)	2.012(18)	5246^{+14}_{-38}	EA
V0719 Aql	19 55 30.6	+07 25 42	11.11	0.350(31)	0.871(22)	9941^{+28}_{-29}	EA
V1345 Aql	19 12 39.2	+05 20 37	13.9	0.396(41)	0.633(16)	–	EA
V1464 Aql	19 50 15.5	-08 36 06	8.62	0.175(33)	4.995(23)	10699^{+36}_{-34}	EW
V1713 Aql	19 37 44.0	+01 49 36	10.61	0.542(33)	5.482(20)	5615^{+58}_{-47}	EW
Y Aql	19 06 58.6	+11 04 16	5.05	-0.006(41)	4.67(63)	–	EB:
KO Ara	17 46 31.0	-53 52 51	12.8	0.490(32)	1.965(17)	5510^{+12}_{-9}	EW
KU Ara	18 01 45.0	-52 34 55	12.3	0.375(34)	1.114(14)	6435^{+16}_{-16}	EA
V0781 Ara	17 07 13.8	-56 56 13	14.5	0.335(40)	0.618(22)	–	E
V0851 Ara	17 07 35.1	-46 40 47	6.93	0.185(30)	10.403(26)	–	EB
V0523 Aur	07 24 03.5	+41 26 02	13.4	0.543(30)	1.775(20)	–	EW
AP Aps	15 44 19.4	-76 15 16	14.4	0.738(32)	0.484(17)	–	EB
AQ Cam	04 51 17.8	+54 56 00	12.0	0.300(30)	0.349(15)	13180^{+2}_{-3}	EA
AW Cam	06 47 28.8	+69 37 45	8.22	0.027(31)	3.371(25)	9438^{+137}_{-222}	EB
DO Cha	09 07 47.2	-82 19 30	7.64	0.317(45)	12.740(18)	6019^{+2}_{-2}	ELL
EQ CMa	06 48 51.6	-16 18 04	12.2	0.751(37)	2.524(20)	–	EA
RU Cnc	08 37 30.1	+23 33 42	10.02	0.603(38)	2.451(16)	6060^{+9}_{-9}	EA/RS
V0388 Cen	12 01 50.2	-45 38 14	13.05	0.781(31)	0.592(27)	4900^{+11}_{-30}	EB

Table 1 *continued on next page*

Light curve analysis

- First, we used all TESS observations to obtain a precise linear ephemeris.

Table 2. Linear ephemeris of studied systems and number of TESS sectors (N_{sec}). T_0 – initial epoch in $BJD - 2400000$, P – period, dP/dt – period change rate. Standard errors are given in parentheses.

System	T_0 [BJD]	P [d]	dP/dt [d·yr^{-1}]	N_{sec}	Note
XZ And	59899.12757 (29)	1.35729906 (77)	—	3	
V0395 And	59875.03733 (78)	0.6846696 (28)	—	2	
BQ Aqr	58360.273 (24)	6.62031 (18)	—	3	(*)
V0719 Aql	60523.8601 (13)	6.75101 (11)	—	2	
V1345 Aql	60494.16382 (32)	3.0283279 (20)	—	2	
V1464 Aql	60526.73129 (11)	0.69783829 (51)	—	2	(*)
V1713 Aql	60507.052162 (46)	0.531730072 (84)	—	2	(b)
Y Aql	59785.75087 (97)	1.302265 (16)	—	2	
KO Ara	60113.46042 (12)	0.382547815 (95)	—	3	(b)
KU Ara	60099.603201 (55)	1.15690574 (23)	—	3	
V0781 Ara	60105.226780 (51)	0.523364785 (90)	—	4	
V0851 Ara	60101.336010 (62)	0.617358284 (70)	—	4	
V0523 Aur	59944.15303 (11)	0.33043925 (11)	—	3	(b)
AP Aps	59364.37412 (40)	2.6890254 (20)	—	4	
AW Car	2460749.9080 (47)	6.51070 (20)	—	7	(a)
AQ Cam	59911.32241 (36)	3.1091177 (22)	—	3	
DO Cha	60062.99914 (83)	0.681454 (12)	$-1.7 \cdot 10^{-5}$ (11)	8	(b)
EQ CMa	60663.4305 (28)	2.2914627 (59)	—	4	(b), (*)
RU Cnc	59558.1273 (88)	10.17290 (21)	—	4	(*)
V0388 Cen	60749.3759 (21)	4.463208 (20)	—	4	
V1054 Cen	60055.4832578 (16)	0.3483075893 (32)	$-3.095 \cdot 10^{-6}$ (21)	3	(b)

Light curve analysis

- For LC analysis, we used the ELISa code (Čokina et al., 2021) — a `Python` package designed for modelling EBs.

- The Levenberg–Marquardt least-squares method was employed to determine the initial approximate solutions. The final set of parameters and their uncertainties were obtained using a Monte Carlo Markov chain sampler.

- The model contains five free parameters: the orbital inclination (i), the photometric mass ratio (q), the surface potentials of both components (Ω_1 and Ω_2), and the effective temperature of the secondary component (T_2).

- The temperature of the primary component, T_1, was adopted from the Gaia DR3 database and was held constant during the fitting routine.

- In the first step, we did not take any stellar spots into account. We assumed a circular orbit for all systems except OR Gem, for which an eccentric orbit was necessary due to the significant offset of the secondary minimum. For contact systems, we used a single common surface potential $\Omega = \Omega_1 = \Omega_2$.

Light curve analysis

Table 3. Photometric elements of the studied systems determined by ELISa code: q – photometric mass ratio, i – inclination, T_2/T_1 – temperature ratio, Ω_1, Ω_2 – surface potentials, Ω_C – critical potential, R_1^{eq}, R_2^{eq} – equivalent radii in units of semi-major axis. Standard errors are given in parentheses.

System	q	i [deg]	T_2/T_1	Ω_1	Ω_2	Ω_C	R_1^{eq} [SMA]	R_2^{eq} [SMA]	Note
XZ And	$1.19905^{+0.0008}_{-0.21524}$	$88.33^{+0.019}_{-1.142}$	$0.644162^{+0.001883}_{-0.000279}$	$4.5465^{+0.0026}_{-0.0642}$	$4.989^{+0.0029}_{-0.556}$	$4.0669^{+0.0012}_{-0.3433}$	$0.30554^{+0.00018}_{-0.00692}$	$0.29827^{+0.00407}_{-0.00014}$	(a)
V0719 Aql	$11.41^{+0.52}_{-0.54}$	$82.066^{+0.095}_{-0.098}$	$0.503028^{+0.000744}_{-0.000493}$	$18.77^{+0.63}_{-0.59}$	$53.5^{+2.0}_{-2.2}$	$16.71^{+0.59}_{-0.62}$	$0.1386^{+0.0016}_{-0.0019}$	$0.1987^{+0.0017}_{-0.0017}$	(a)
V1345 Aql	$1.039^{+0.044}_{-0.066}$	$80.64^{+0.28}_{-0.18}$	$0.65207^{+0.00362}_{-0.00241}$	$5.364^{+0.078}_{-0.113}$	$5.52^{+0.12}_{-0.22}$	$3.814^{+0.071}_{-0.108}$	$0.2335^{+0.0032}_{-0.0024}$	$0.2317^{+0.0022}_{-0.0033}$	(a), (b)
Y Aql	$0.64968^{+0.00025}_{-0.01956}$	$50.32^{+0.04}_{-0.061}$	$0.4867765^{+0.0000559}_{-0.0085488}$	$4.5112^{+0.0015}_{-0.0447}$	$4.6484^{+0.0021}_{-0.063}$	$3.15365^{+0.00046}_{-0.0353}$	$0.261494^{+0.001765}_{-9e-05}$	$0.188023^{+8.2e-05}_{-0.001229}$	(a)
KU Ara	$0.712^{+0.061}_{-0.04}$	$70.42^{+0.42}_{-0.21}$	$0.55730^{+0.01134}_{-0.00280}$	$4.554^{+0.113}_{-0.082}$	$3.455^{+0.31}_{-0.091}$	$3.264^{+0.106}_{-0.07}$	$0.2628^{+0.0036}_{-0.004}$	$0.3186^{+0.0039}_{-0.0068}$	
AW Car	$0.901^{+0.066}_{-0.057}$	$84.79^{+0.34}_{-0.67}$	$0.46319^{+0.00602}_{-0.00374}$	$5.438^{+0.112}_{-0.097}$	$8.2^{+0.42}_{-0.62}$	$3.587^{+0.109}_{-0.096}$	$0.2224^{+0.0019}_{-0.0024}$	$0.1266^{+0.0043}_{-0.0021}$	(c)
AQ Cam	$0.87^{+0.0081}_{-0.2341}$	$86.19^{+2.11}_{-0.27}$	$0.42564^{+0.00235}_{-0.00402}$	$4.776^{+0.03}_{-0.299}$	$4.985^{+0.013}_{-0.98}$	$3.535^{+0.014}_{-0.407}$	$0.2586^{+0.0063}_{-0.0014}$	$0.2246^{+0.002}_{-0.007}$	(a)
V1133 Cen	$0.77^{+0.16}_{-0.2}$	$79.9^{+6.3}_{-8.1}$	$0.6082^{+0.0289}_{-0.0123}$	$4.16^{+0.65}_{-0.45}$	$3.86^{+0.53}_{-0.56}$	$3.37^{+0.28}_{-0.35}$	$0.303^{+0.022}_{-0.042}$	$0.2838^{+0.0212}_{-0.0067}$	(a), (c)
DL Cep	$0.958^{+0.038}_{-0.213}$	$84.0^{+0.69}_{-0.17}$	$0.64868^{+0.00743}_{-0.00438}$	$3.974^{+0.038}_{-0.205}$	$3.904^{+0.09}_{-0.401}$	$3.682^{+0.061}_{-0.359}$	$0.3434^{+0.0041}_{-0.0047}$	$0.3445^{+0.0041}_{-0.0244}$	
TV Cep	$0.2207^{+0.2511}_{-0.0025}$	$85.27^{+0.32}_{-0.39}$	$0.58333^{+0.03895}_{-0.00185}$	$8.413^{+0.059}_{-1.709}$	$2.3054^{+1.0572}_{-0.0067}$	$2.2836^{+0.5377}_{-0.0062}$	$0.1221^{+0.03933}_{-0.00087}$	$0.2498^{+0.0011}_{-0.0038}$	(a)
KL Cas	$2.2^{+0.131}_{-0.044}$	$86.999^{+0.057}_{-0.135}$	$0.580688^{+0.002130}_{-0.000575}$	$5.75^{+0.267}_{-0.057}$	$7.67^{+0.22}_{-0.12}$	$5.532^{+0.181}_{-0.061}$	$0.2905^{+0.0012}_{-0.0064}$	$0.30694^{+0.00267}_{-0.00055}$	(a), (b)
AQ Cir	$0.86^{+0.14}_{-0.2}$	$76.91^{+2.19}_{-0.3}$	$0.74211^{+0.00180}_{-0.01779}$	$3.67^{+0.18}_{-0.37}$	$3.72^{+0.15}_{-0.37}$	$3.51^{+0.23}_{-0.35}$	$0.3702^{+0.0284}_{-0.0074}$	$0.347^{+0.013}_{-0.04}$	(a)
TW Cir	$0.913^{+0.07}_{-0.078}$	$68.18^{+4.17}_{-0.38}$	$0.68982^{+0.01789}_{-0.00316}$	$3.82^{+0.17}_{-0.12}$	$3.68^{+0.47}_{-0.13}$	$3.61^{+0.12}_{-0.13}$	$0.3571^{+0.0072}_{-0.0092}$	$0.3652^{+0.0064}_{-0.0625}$	(a)
DT Cru	$0.924^{+0.054}_{-0.312}$	$45.47^{+4.17}_{-0.34}$	$0.98899^{+0.00292}_{-0.00235}$	$3.414^{+0.067}_{-0.302}$		$3.626^{+0.088}_{-0.539}$	$0.4311^{+0.0116}_{-0.005}$	$0.4188^{+0.006}_{-0.0585}$	(a)
SX Cru	$1.77^{+0.14}_{-0.33}$	$86.9^{+0.55}_{-0.83}$	$0.61316^{+0.00401}_{-0.00455}$	$5.24^{+0.18}_{-0.29}$	$5.45^{+0.3}_{-0.51}$	$4.92^{+0.2}_{-0.49}$	$0.2966^{+0.0043}_{-0.0035}$	$0.3793^{+0.0022}_{-0.0043}$	(a)
CV Cyg	$0.2261^{+0.24398}_{-0.00023}$	$81.098^{+0.049}_{-8.881}$	$1.025654^{+0.000201}_{-0.012758}$	$2.21022^{+0.51129}_{-0.00085}$		$2.29645^{+0.52144}_{-0.00056}$	$0.54226^{+0.00022}_{-0.05998}$	$0.29273^{+0.04659}_{-0.00012}$	(a)
PV Cyg	$0.707^{+0.142}_{-0.098}$	$76.17^{+1.18}_{-0.83}$	$0.62005^{+0.00886}_{-0.00978}$	$4.13^{+0.34}_{-0.26}$	$3.87^{+0.47}_{-0.37}$	$3.26^{+0.24}_{-0.18}$	$0.3^{+0.014}_{-0.026}$	$0.273^{+0.015}_{-0.026}$	(c)
QU Cyg	$1.34^{+0.027}_{-0.042}$	$89.5^{+0.36}_{-2.25}$	$0.95023^{+0.00207}_{-0.00207}$	$4.201^{+0.042}_{-0.056}$		$4.285^{+0.042}_{-0.065}$	$0.3675^{+0.0026}_{-0.002}$	$0.4189^{+0.0024}_{-0.0031}$	(a),(b)
V0445 Cyg	$0.3277^{+0.0846}_{-0.0047}$	$86.641^{+0.087}_{-0.169}$	$0.582701^{+0.003135}_{-0.000770}$	$5.586^{+0.021}_{-0.026}$	$2.619^{+0.43}_{-0.016}$	$2.527^{+0.176}_{-0.01}$	$0.19074^{+0.00243}_{-0.00063}$	$0.26316^{+0.00034}_{-0.00894}$	(a)
V0703 Cyg	$1.472^{+0.027}_{-0.653}$	$85.44^{+0.094}_{-17.642}$	$0.67267^{+0.17248}_{-0.00208}$	$6.33^{+1.04}_{-0.14}$	$7.751^{+0.066}_{-2.617}$	$4.484^{+0.04}_{-1.035}$	$0.2081^{+0.0012}_{-0.0519}$	$0.2137^{+0.0192}_{-0.0011}$	(a)
V0825 Cyg	$0.61^{+0.18}_{-0.16}$	$80.0^{+3.6}_{-5.2}$	$0.4292^{+0.0457}_{-0.0302}$	$4.37^{+0.49}_{-0.38}$	$4.04^{+0.8}_{-0.69}$	$3.08^{+0.32}_{-0.3}$	$0.271^{+0.019}_{-0.026}$	$0.224^{+0.03}_{-0.048}$	(c)
V0959 Cyg	$0.55^{+0.228}_{-0.039}$	$86.137^{+0.024}_{-0.011}$	$0.993818^{+0.000575}_{-0.002444}$	$9.32^{+0.19}_{-0.11}$	$6.04^{+2.07}_{-0.31}$	$2.972^{+0.408}_{-0.074}$	$0.1142^{+0.0018}_{-0.0012}$	$0.1142^{+0.0012}_{-0.0018}$	(a) / (b)
V1374 Cyg	$0.951^{+0.039}_{-0.076}$	$72.61^{+0.31}_{-0.22}$	$0.93971^{+0.00290}_{-0.00268}$	$3.7^{+0.053}_{-0.098}$	$3.768^{+0.081}_{-0.14}$	$3.669^{+0.063}_{-0.126}$	$0.38^{+0.0052}_{-0.0057}$	$0.3595^{+0.0074}_{-0.0078}$	(a)
V1433 Cyg	$0.521^{+0.187}_{-0.078}$	$80.49^{+0.78}_{-7.71}$	$0.4944^{+0.0418}_{-0.0103}$	$4.51^{+0.62}_{-0.16}$	$4.27^{+1.07}_{-0.41}$	$2.92^{+0.34}_{-0.15}$	$0.2511^{+0.0056}_{-0.0243}$	$0.1667^{+0.0134}_{-0.0099}$	
VV Cyg	$0.599^{+0.175}_{-0.014}$	$81.94^{+1.18}_{-0.16}$	$0.63263^{+0.00380}_{-0.01015}$	$4.54^{+0.52}_{-0.11}$	$3.077^{+0.994}_{-0.038}$	$3.061^{+0.31}_{-0.026}$	$0.256^{+0.021}_{-0.023}$	$0.3341^{+0.004}_{-0.0343}$	
EL Gem	$0.543^{+0.049}_{-0.158}$	$86.36^{+0.72}_{-6.03}$	$1.00036^{+0.00170}_{-0.00742}$	$3.937^{+0.07}_{-0.308}$	$3.192^{+0.062}_{-0.33}$	$2.957^{+0.092}_{-0.311}$	$0.2996^{+0.0121}_{-0.0032}$	$0.2915^{+0.0065}_{-0.0446}$	(c)
IP Gem	$0.994^{+0.0046}_{-0.0254}$	$84.45^{+0.24}_{-0.27}$	$0.77054^{+0.00146}_{-0.00157}$	$3.852^{+0.0076}_{-0.0305}$	$5.222^{+0.029}_{-0.104}$	$3.7403^{+0.0075}_{-0.0414}$	$0.36287^{+0.00111}_{-0.00068}$	$0.2376^{+0.0014}_{-0.0011}$	(a)
OR Gem	$0.81^{+0.15}_{-0.19}$	$84.41^{+0.44}_{-0.4}$	$0.98547^{+0.00184}_{-0.00346}$	$5.9^{+0.35}_{-0.82}$	$4.7^{+0.38}_{-0.56}$	$3.49^{+0.26}_{-0.34}$	$0.198^{+0.0277}_{-0.0087}$	$0.2345^{+0.0066}_{-0.0239}$	(d)
UW Gem	$1.01^{+0.19}_{-0.14}$	$76.48^{+0.91}_{-1.67}$	$0.5632^{+0.0559}_{-0.0279}$	$5.79^{+2.24}_{-0.48}$	$5.61^{+0.96}_{-1.5}$	$3.77^{+0.3}_{-0.23}$	$0.219^{+0.013}_{-0.077}$	$0.216^{+0.088}_{-0.016}$	(a), (c)
WY Hor	$0.7968^{+0.003}_{-0.1747}$	$41.6^{+11.7}_{-1.6}$	$0.86344^{+0.00265}_{-0.03320}$	$2.9808^{+0.0063}_{-0.074}$		$3.4116^{+0.0052}_{-0.3078}$	$0.5002^{+0.00043}_{-0.02039}$	$0.4637^{+0.0014}_{-0.0656}$	(a),(c)
VW Hya	$1.629^{+0.019}_{-0.207}$	$85.516^{+0.027}_{-0.095}$	$0.399364^{+0.017985}_{-0.000901}$	$6.491^{+0.031}_{-0.037}$	$7.034^{+0.065}_{-0.75}$	$4.716^{+0.028}_{-0.308}$	$0.20738^{+0.00037}_{-0.00316}$	$0.25898^{+0.00156}_{-0.00019}$	(a)
XX Lac	$0.936^{+0.074}_{-0.272}$	$84.68^{+0.48}_{-3.48}$	$0.69431^{+0.04885}_{-0.00383}$	$4.81^{+0.75}_{-0.11}$	$5.29^{+0.29}_{-1.65}$	$3.64^{+0.12}_{-0.47}$	$0.2654^{+0.0036}_{-0.0563}$	$0.2249^{+0.043}_{-0.0032}$	
WX Lep	$0.58964^{+0.00033}_{-0.02022}$	$47.411^{+0.068}_{-0.432}$	$0.523858^{+0.000327}_{-0.004259}$	$3.16232^{+0.00063}_{-0.05414}$	$3.04472^{+0.00032}_{-0.01412}$	$3.04439^{+0.00061}_{-0.03741}$	$0.403966^{+0.006204}_{-7.6e-05}$	$0.334273^{+5e-05}_{-0.004978}$	(a)
V0401 Lyr	$1.23^{+0.073}_{-0.185}$	$85.45^{+0.27}_{-0.35}$	$0.52283^{+0.00243}_{-0.00672}$	$5.43^{+0.12}_{-0.2}$	$6.32^{+0.27}_{-0.66}$	$4.11^{+0.11}_{-0.29}$	$0.2411^{+0.0035}_{-0.0028}$	$0.2283^{+0.0019}_{-0.0019}$	(a)
V0417 Lyr	$0.79^{+0.14}_{-0.13}$	$75.03^{+0.39}_{-0.29}$	$1.00690^{+0.00517}_{-0.00366}$	$3.56^{+0.26}_{-0.22}$	$3.47^{+0.39}_{-0.27}$	$3.4^{+0.24}_{-0.22}$	$0.378^{+0.013}_{-0.02}$	$0.349^{+0.016}_{-0.016}$	(a)

Light curve analysis

Table 4. Photometric elements of the studied systems with significant star spots determined by ELISa code: q – photometric mass ratio, i – inclination, T_2/T_1 – temperature ratio, Ω_1, Ω_2 – surface potentials, Ω_C – critical potential, R_1^{eq}, R_2^{eq} – equivalent radii in units of semi-major axis. Parameters of spot are given in Tab. 5. Standard errors are given in parentheses.

System	q	i [deg]	T_2/T_1	Ω_1	Ω_2	Ω_C	R_1^{eq} [SMA]	R_2^{eq} [SMA]	Note
V0395 And	$0.762^{+0.047}_{-0.048}$	$56.5^{+2.2}_{-3.6}$	$0.8255^{+0.0230}_{-0.0364}$	$4.34^{+0.59}_{-0.18}$	$4.79^{+0.51}_{-0.67}$	$3.351^{+0.081}_{-0.084}$	$0.284^{+0.013}_{-0.043}$	$0.213^{+0.046}_{-0.032}$	
AP Aps	$0.757^{+0.157}_{-0.019}$	$89.02^{+0.52}_{-5.08}$	$0.88163^{+0.00756}_{-0.00176}$	$5.587^{+0.033}_{-0.315}$	$3.345^{+0.333}_{-0.034}$	$3.343^{+0.266}_{-0.033}$	$0.208^{+0.0243}_{-0.0018}$	$0.3545^{+0.0067}_{-0.0024}$	
V1713 Aql	$1.19902^{+0.00083}_{-0.11734}$	$69.435^{+0.023}_{-0.02}$	$0.950988^{+0.000321}_{-0.006768}$	$4.0206^{+0.0013}_{-0.162}$		$4.0669^{+0.0013}_{-0.1853}$	$0.3715^{+0.00719}_{-0.00015}$	$0.4033^{+0.00019}_{-0.00813}$	
KO Ara	$1.171^{+0.024}_{-0.222}$	$75.63^{+0.31}_{-0.74}$	$0.93096^{+0.00149}_{-0.00535}$	$3.967^{+0.026}_{-0.347}$		$4.023^{+0.037}_{-0.357}$	$0.3761^{+0.0189}_{-0.0014}$	$0.4035^{+0.0034}_{-0.0163}$	
V0781 Ara	$1.124^{+0.061}_{-0.198}$	$57.56^{+1.42}_{-0.3}$	$0.85379^{+0.00418}_{-0.00509}$	$4.201^{+0.089}_{-0.297}$	$4.044^{+0.082}_{-0.246}$	$3.948^{+0.096}_{-0.32}$	$0.3357^{+0.0124}_{-0.0053}$	$0.3789^{+0.0055}_{-0.0285}$	
V0851 Ara	$0.898^{+0.053}_{-0.038}$	$49.44^{+0.87}_{-1.27}$	$0.98911^{+0.00316}_{-0.01936}$	$3.734^{+0.11}_{-0.063}$	$4.34^{+0.23}_{-0.55}$	$3.582^{+0.087}_{-0.064}$	$0.3665^{+0.0055}_{-0.0091}$	$0.2765^{+0.048}_{-0.0051}$	(a)
V0523 Aur	$0.98^{+0.015}_{-0.07}$	$81.836^{+0.075}_{-0.072}$	$0.96203^{+0.00171}_{-0.00102}$	$3.697^{+0.025}_{-0.119}$		$3.717^{+0.025}_{-0.116}$	$0.3853^{+0.0069}_{-0.0014}$	$0.3818^{+0.0013}_{-0.0056}$	
V0442 Cas	$0.812^{+0.175}_{-0.01}$	$84.558^{+0.247}_{-0.086}$	$0.48575^{+0.00681}_{-0.00120}$	$7.622^{+0.066}_{-0.032}$	$4.31^{+0.671}_{-0.037}$	$3.437^{+0.292}_{-0.018}$	$0.14748^{+0.00172}_{-0.0008}$	$0.25546^{+0.00068}_{-0.00242}$	
V0388 Cen	$0.96^{+0.16}_{-0.17}$	$84.82^{+0.78}_{-0.61}$	$0.9823^{+0.0120}_{-0.0322}$	$4.28^{+0.31}_{-0.18}$	$3.98^{+1.06}_{-0.42}$	$3.69^{+0.25}_{-0.28}$	$0.293^{+0.053}_{-0.014}$	$0.333^{+0.012}_{-0.054}$	
V1054 Cen	$0.99908^{+0.00076}_{-0.06789}$	$85.09^{+0.028}_{-0.051}$	$0.984183^{+0.000496}_{-0.001117}$	$3.6848^{+0.0014}_{-0.1041}$		$3.7485^{+0.0012}_{-0.1112}$	$0.39126^{+0.00549}_{-0.00019}$	$0.391^{+0.00019}_{-0.00416}$	
DO Cha	$0.888^{+0.049}_{-0.032}$	$53.8^{+1.3}_{-1.0}$	$0.82305^{+0.01927}_{-0.00366}$	$4.351^{+0.178}_{-0.084}$	$4.59^{+0.19}_{-0.33}$	$3.566^{+0.082}_{-0.054}$	$0.2946^{+0.0047}_{-0.0127}$	$0.2555^{+0.0268}_{-0.0087}$	
EQ Com	$1.113^{+0.064}_{-0.185}$	$68.57^{+0.14}_{-0.12}$	$1.00530^{+0.00614}_{-0.08912}$	$3.981^{+0.079}_{-0.337}$	$3.981^{+0.079}_{-0.337}$	$3.93^{+0.1}_{-0.3}$	$0.365^{+0.0212}_{-0.0032}$	$0.3868^{+0.0044}_{-0.017}$	
OV Cyg	$0.879^{+0.087}_{-0.071}$	$81.5^{+1.0}_{-6.1}$	$0.6443^{+0.0604}_{-0.0141}$	$4.44^{+1.57}_{-0.11}$	$6.64^{+0.57}_{-1.84}$	$3.55^{+0.14}_{-0.12}$	$0.2852^{+0.0042}_{-0.0888}$	$0.1502^{+0.0956}_{-0.0063}$	
V0706 Cyg	$0.9947^{+0.0041}_{-0.0723}$	$76.8^{+0.289}_{-0.047}$	$0.87122^{+0.00171}_{-0.00228}$	$3.7823^{+0.0096}_{-0.1148}$	$3.7482^{+0.0072}_{-0.089}$	$3.7414^{+0.0066}_{-0.1186}$	$0.3735^{+0.0065}_{-0.001}$	$0.37798^{+0.001}_{-0.00951}$	
V2082 Cyg	$0.8051^{+0.0868}_{-0.0043}$	$43.122^{+2.131}_{-0.099}$	$0.87285^{+0.01528}_{-0.00100}$	$3.3279^{+0.1606}_{-0.0086}$		$3.4257^{+0.1464}_{-0.0074}$	$0.4186^{+0.00068}_{-0.01147}$	$0.3808^{+0.00632}_{-0.00065}$	(a)
BR Dra	$0.785^{+0.079}_{-0.099}$	$82.02^{+0.64}_{-1.52}$	$0.78247^{+0.00689}_{-0.00672}$	$3.95^{+0.15}_{-0.15}$	$4.54^{+0.36}_{-0.45}$	$3.39^{+0.13}_{-0.17}$	$0.3238^{+0.0053}_{-0.0093}$	$0.2284^{+0.011}_{-0.0061}$	
AN Eri	$1.068^{+0.04}_{-0.035}$	$64.21^{+1.36}_{-0.11}$	$0.89982^{+0.00310}_{-0.01823}$	$3.867^{+0.077}_{-0.054}$	$3.873^{+0.12}_{-0.055}$	$3.86^{+0.063}_{-0.057}$	$0.3732^{+0.0029}_{-0.0054}$	$0.3846^{+0.0027}_{-0.0111}$	
HL Eri	$0.751^{+0.024}_{-0.022}$	$45.37^{+7.87}_{-0.27}$	$0.5747^{+0.0429}_{-0.0214}$	$4.123^{+0.101}_{-0.061}$	$3.396^{+0.504}_{-0.071}$	$3.332^{+0.042}_{-0.039}$	$0.3014^{+0.0041}_{-0.0073}$	$0.3439^{+0.0083}_{-0.0664}$	
V1003 Her	$1.0464^{+0.0028}_{-0.0527}$	$42.91^{+3.92}_{-0.96}$	$0.92968^{+0.00276}_{-0.00303}$	$3.2816^{+0.0145}_{-0.0061}$		$3.8251^{+0.0046}_{-0.0852}$	$0.49332^{+0.00037}_{-0.01727}$	$0.50003^{+0.00027}_{-0.02499}$	(a)
SZ Hor	$1.031^{+0.066}_{-0.085}$	$75.09^{+2.8}_{-0.31}$	$0.75758^{+0.00952}_{-0.00129}$	$3.84^{+0.087}_{-0.13}$	$3.86^{+0.23}_{-0.13}$	$3.8^{+0.11}_{-0.14}$	$0.3741^{+0.0065}_{-0.0044}$	$0.3806^{+0.0072}_{-0.0627}$	
CH Hya	$1.187^{+0.01}_{-0.199}$	$82.14^{+0.14}_{-0.16}$	$0.94401^{+0.00198}_{-0.00342}$	$3.982^{+0.015}_{-0.267}$		$4.049^{+0.016}_{-0.318}$	$0.3759^{+0.0122}_{-0.0011}$	$0.4059^{+0.001}_{-0.0144}$	
CE Hyi	$1.091^{+0.09}_{-0.102}$	$43.1^{+4.2}_{-2.1}$	$0.9146^{+0.0184}_{-0.0307}$	$3.804^{+0.066}_{-0.131}$		$3.9^{+0.14}_{-0.16}$	$0.3922^{+0.0084}_{-0.0139}$	$0.4^{+0.028}_{-0.011}$	(a)
V0884 Mon	$0.94^{+0.12}_{-0.13}$	$59.0^{+6.0}_{-6.3}$	$0.6624^{+0.0330}_{-0.0382}$	$5.92^{+0.65}_{-0.53}$	$5.44^{+0.8}_{-0.81}$	$3.65^{+0.2}_{-0.21}$	$0.202^{+0.022}_{-0.021}$	$0.213^{+0.041}_{-0.026}$	(a)
IT Nor	$0.74^{+0.27}_{-0.12}$	$69.24^{+0.78}_{-1.15}$	$0.70839^{+0.00131}_{-0.00171}$	$3.23^{+0.47}_{-0.21}$		$3.31^{+0.46}_{-0.21}$	$0.422^{+0.017}_{-0.031}$	$0.366^{+0.024}_{-0.012}$	
V0389 Nor	$1.164^{+0.028}_{-0.188}$	$77.773^{+0.093}_{-0.096}$	$0.98619^{+0.00137}_{-0.00473}$	$4.031^{+0.041}_{-0.278}$	$4.031^{+0.041}_{-0.278}$	$4.012^{+0.044}_{-0.301}$	$0.3641^{+0.0129}_{-0.0019}$	$0.3914^{+0.002}_{-0.0169}$	
DE Oct	$0.925^{+0.018}_{-0.02}$	$47.65^{+0.27}_{-1.11}$	$0.83582^{+0.00840}_{-0.00168}$	$3.906^{+0.032}_{-0.115}$	$3.636^{+0.031}_{-0.031}$	$3.628^{+0.029}_{-0.033}$	$0.3455^{+0.0131}_{-0.002}$	$0.3728^{+0.0018}_{-0.0035}$	
BQ Phe	$0.9034^{+0.0315}_{-0.0028}$	$52.2^{+0.15}_{-0.95}$	$0.979408^{+0.000506}_{-0.000196}$	$3.5913^{+0.0745}_{-0.0047}$		$3.5912^{+0.0521}_{-0.0047}$	$0.38881^{+0.00027}_{-0.00489}$	$0.37072^{+0.00263}_{-0.00017}$	
V1276 Sgr	$0.655^{+0.041}_{-0.034}$	$81.2^{+1.3}_{-1.4}$	$0.83730^{+0.00909}_{-0.00152}$	$3.283^{+0.085}_{-0.065}$	$3.61^{+0.2}_{-0.1}$	$3.164^{+0.073}_{-0.061}$	$0.3957^{+0.0049}_{-0.0072}$	$0.271^{+0.015}_{-0.013}$	
BW Vel	$0.803^{+0.07}_{-0.046}$	$77.14^{+0.43}_{-0.31}$	$0.80327^{+0.00854}_{-0.00119}$	$3.446^{+0.207}_{-0.082}$	$3.445^{+0.229}_{-0.086}$	$3.423^{+0.119}_{-0.079}$	$0.3961^{+0.0055}_{-0.0188}$	$0.3561^{+0.0042}_{-0.0067}$	
OQ Vel	$0.952^{+0.07}_{-0.09}$	$49.5^{+5.2}_{-2.8}$	$0.9622^{+0.0121}_{-0.0100}$	$4.32^{+0.39}_{-0.12}$	$4.98^{+0.28}_{-0.61}$	$3.67^{+0.11}_{-0.15}$	$0.3056^{+0.0067}_{-0.0366}$	$0.2415^{+0.0361}_{-0.0062}$	
MW Vir	$0.877^{+0.067}_{-0.019}$	$46.4^{+3.9}_{-2.3}$	$0.87438^{+0.00703}_{-0.00372}$	$4.146^{+0.079}_{-0.062}$	$4.108^{+0.105}_{-0.09}$	$3.547^{+0.111}_{-0.032}$	$0.3137^{+0.0053}_{-0.0086}$	$0.299^{+0.0057}_{-0.0104}$	

NOTE— (a) additional light in the system.

Light curve analysis

Table 4. Photometric elements of the studied systems with si
i – inclination, T_2/T_1 – temperature ratio, Ω_1, Ω_2 – surface
semi-major axis. Parameters of spot are given in Tab. 5. Stan

System	q	i [deg]	T_2/T_1	
V0395 And	$0.762^{+0.047}_{-0.048}$	$56.5^{+2.2}_{-3.6}$	$0.8255^{+0.0230}_{-0.0364}$	4
AP Aps	$0.757^{+0.157}_{-0.019}$	$89.02^{+0.52}_{-5.08}$	$0.88163^{+0.00756}_{-0.00176}$	5.
V1713 Aql	$1.19902^{+0.00083}_{-0.11734}$	$69.435^{+0.023}_{-0.02}$	$0.950988^{+0.000321}_{-0.006768}$	
KO Ara	$1.171^{+0.024}_{-0.222}$	$75.63^{+0.31}_{-0.74}$	$0.93096^{+0.00149}_{-0.00535}$	
V0781 Ara	$1.124^{+0.061}_{-0.198}$	$57.56^{+1.42}_{-0.3}$	$0.85379^{+0.00418}_{-0.00509}$	4.
V0851 Ara	$0.898^{+0.053}_{-0.038}$	$49.44^{+0.87}_{-1.27}$	$0.98911^{+0.00316}_{-0.01936}$	3.
V0523 Aur	$0.98^{+0.015}_{-0.07}$	$81.836^{+0.075}_{-0.072}$	$0.96203^{+0.00171}_{-0.00102}$	
V0442 Cas	$0.812^{+0.175}_{-0.01}$	$84.558^{+0.247}_{-0.086}$	$0.48575^{+0.00681}_{-0.00120}$	7.
V0388 Cen	$0.96^{+0.16}_{-0.17}$	$84.82^{+0.78}_{-0.61}$	$0.9823^{+0.0120}_{-0.0322}$	4
V1054 Cen	$0.99908^{+0.00076}_{-0.06789}$	$85.09^{+0.028}_{-0.051}$	$0.984183^{+0.000496}_{-0.001117}$	
DO Cha	$0.888^{+0.049}_{-0.032}$	$53.8^{+1.3}_{-1.0}$	$0.82305^{+0.01927}_{-0.00366}$	4.
EQ Com	$1.113^{+0.064}_{-0.185}$	$68.57^{+0.14}_{-0.12}$	$1.00530^{+0.00614}_{-0.08912}$	3.
OV Cyg	$0.879^{+0.087}_{-0.071}$	$81.5^{+1.0}_{-6.1}$	$0.6443^{+0.0604}_{-0.0141}$	4
V0706 Cyg	$0.9947^{+0.0041}_{-0.0723}$	$76.8^{+0.289}_{-0.047}$	$0.87122^{+0.00171}_{-0.00228}$	3.78
V2082 Cyg	$0.8051^{+0.0868}_{-0.0043}$	$43.122^{+2.131}_{-0.099}$	$0.87285^{+0.01528}_{-0.00100}$	
BR Dra	$0.785^{+0.079}_{-0.099}$	$82.02^{+0.64}_{-1.52}$	$0.78247^{+0.00689}_{-0.00672}$	3
AN Eri	$1.068^{+0.04}_{-0.035}$	$64.21^{+1.36}_{-0.11}$	$0.89982^{+0.00310}_{-0.01823}$	3.
HL Eri	$0.751^{+0.024}_{-0.022}$	$45.37^{+7.87}_{-0.27}$	$0.5747^{+0.0429}_{-0.0214}$	4.
V1003 Her	$1.0464^{+0.0028}_{-0.0527}$	$42.91^{+3.92}_{-0.96}$	$0.92968^{+0.00276}_{-0.00303}$	
SZ Hor	$1.031^{+0.066}_{-0.085}$	$75.09^{+2.8}_{-0.31}$	$0.75758^{+0.00952}_{-0.00129}$	3.
CH Hya	$1.187^{+0.01}_{-0.199}$	$82.14^{+0.14}_{-0.16}$	$0.94401^{+0.00198}_{-0.00342}$	
CE Hyi	$1.091^{+0.09}_{-0.102}$	$43.1^{+4.2}_{-2.1}$	$0.9146^{+0.0184}_{-0.0307}$	
V0884 Mon	$0.94^{+0.12}_{-0.13}$	$59.0^{+6.0}_{-6.3}$	$0.6624^{+0.0330}_{-0.0382}$	5
IT Nor	$0.74^{+0.27}_{-0.12}$	$69.24^{+0.78}_{-1.15}$	$0.70839^{+0.00131}_{-0.00171}$	
V0389 Nor	$1.164^{+0.028}_{-0.188}$	$77.773^{+0.093}_{-0.096}$	$0.98619^{+0.00137}_{-0.00473}$	4.
DE Oct	$0.925^{+0.018}_{-0.02}$	$47.65^{+0.27}_{-1.11}$	$0.83582^{+0.00840}_{-0.00168}$	3.
BQ Phe	$0.9034^{+0.0315}_{-0.0028}$	$52.2^{+0.15}_{-0.95}$	$0.979408^{+0.000506}_{-0.000196}$	
V1276 Sgr	$0.655^{+0.041}_{-0.034}$	$81.2^{+1.3}_{-1.4}$	$0.83730^{+0.00909}_{-0.00152}$	3.
BW Vel	$0.803^{+0.07}_{-0.046}$	$77.14^{+0.43}_{-0.31}$	$0.80327^{+0.00854}_{-0.00119}$	3.
OQ Vel	$0.952^{+0.07}_{-0.09}$	$49.5^{+5.2}_{-2.8}$	$0.9622^{+0.0121}_{-0.0100}$	4
MW Vir	$0.877^{+0.067}_{-0.019}$	$46.4^{+3.9}_{-2.3}$	$0.87438^{+0.00703}_{-0.00372}$	4.

NOTE— (a) additional light in the system.

Table 5. Parameters of spot on the studied systems from Tab. 4 determined by ELISa code: r_s – spot radius, $T_s/T_\star$ – temperature factor, φ_s – spot latitude, ϑ_s – spot longitude. Standard errors are given in parentheses.

System	Spot loc.	r_s [deg]	$T_s/T_\star$	φ_s [deg]	ϑ_s [deg]
V0395 And	prim	$8.8^{+6.8}_{-1.7}$	0.59	$178.7^{+11.6}_{-2.4}$	$124.0^{+18.0}_{-10.0}$
AP Aps	sec	$34.78^{+0.67}_{-1.69}$	0.91	$62.2^{+15.7}_{-1.9}$	$71.7^{+1.4}_{-3.0}$
V1713 Aql	sec	$18.49^{+0.32}_{-0.98}$	0.79	$128.43^{+1.46}_{-0.81}$	$119.939^{+0.052}_{-15.851}$
KO Ara	sec	$31.8^{+12.2}_{-1.7}$	0.89	$57.0^{+23.0}_{-31.0}$	$263.8^{+1.8}_{-9.9}$
V0781 Ara	sec	$17.7^{+1.5}_{-2.6}$	0.8	$112.2^{+4.8}_{-3.7}$	$246.5^{+4.4}_{-3.2}$
V0851 Ara	prim	$7.46^{+2.24}_{-0.43}$	0.73	$266.7^{+2.7}_{-25.2}$	$104.9^{+9.5}_{-4.3}$
V0523 Aur	sec	$49.85^{+0.12}_{-3.41}$	0.79	$149.91^{+0.072}_{-5.168}$	$232.9^{+1.0}_{-1.5}$
V0442 Cas	sec	$39.76^{+0.21}_{-12.95}$	0.79	$147.32^{+0.78}_{-24.93}$	$47.4^{+8.6}_{-1.8}$
V0388 Cen	sec	$38.8^{+9.3}_{-5.0}$	0.93	$96.0^{+20.0}_{-17.0}$	$202.7^{+33.7}_{-3.4}$
V1054 Cen	sec	$14.93^{+2.12}_{-0.25}$	0.78	$104.0^{+17.8}_{-3.5}$	$271.6^{+0.87}_{-0.99}$
DO Cha	sec	$18.2^{+2.2}_{-1.0}$	0.89	$122.1^{+3.5}_{-2.1}$	$128.4^{+1.5}_{-15.8}$
EQ Com	sec	$69.82^{+0.15}_{-8.88}$	0.91	$50.8^{+28.87}_{-0.7}$	$227.08^{+20.25}_{-0.69}$
OV Cyg	prim	$9.9^{+4.0}_{-1.5}$	0.77	$242.0^{+13.0}_{-19.0}$	$84.0^{+32.0}_{-43.0}$
V0706 Cyg	sec	$38.8^{+2.5}_{-3.2}$	0.8	$126.4^{+3.3}_{-6.1}$	$75.26^{+0.89}_{-2.91}$
V2082 Cyg	sec	$41.8^{+2.3}_{-5.8}$	0.75	$111.7^{+3.2}_{-4.8}$	$280.2^{+0.19}_{-0.88}$
BR Dra	sec	$41.4^{+17.0}_{-4.7}$	0.91	$86.0^{+39.0}_{-47.0}$	$93.0^{+40.0}_{-17.0}$
AN Eri	sec	$103.29^{+0.6}_{-9.08}$	0.87	$55.8^{+2.0}_{-4.0}$	$222.6^{+3.87}_{-0.48}$
HL Eri	sec	$53.97^{+0.91}_{-8.76}$	0.9	$95.0^{+8.9}_{-4.9}$	$11.13^{+2.35}_{-0.41}$
V1003 Her	prim	$15.48^{+0.94}_{-1.0}$	0.73	$275.8^{+6.9}_{-3.0}$	$100.9^{+2.3}_{-2.9}$
SZ Hor	sec	$22.2^{+1.6}_{-10.4}$	0.87	$131.5^{+16.2}_{-6.5}$	$295.8^{+3.8}_{-57.6}$
CH Hya	sec	$20.1^{+1.8}_{-1.5}$	0.89	$64.0^{+40.0}_{-14.0}$	$290.5^{+4.3}_{-6.4}$
CE Hyi	sec	$21.5^{+4.1}_{-2.5}$	0.85	$96.4^{+9.1}_{-5.2}$	$265.1^{+5.2}_{-2.0}$
V0884 Mon	prim	$8.6^{+7.3}_{-2.7}$	0.65	$223.0^{+52.0}_{-12.0}$	$118.0^{+21.0}_{-28.0}$
IT Nor	prim	$13.08^{+2.0}_{-0.15}$	0.69	$101.38^{+0.65}_{-0.58}$	$94.0^{+8.9}_{-2.3}$
V0389 Nor	sec	$19.09^{+0.51}_{-0.47}$	0.89	$73.3^{+10.4}_{-4.6}$	$294.5^{+2.3}_{-7.7}$
DE Oct	prim	$8.601^{+1.037}_{-0.093}$	0.8	$246.8^{+5.7}_{-1.3}$	$90.4^{+9.83}_{-0.32}$
BQ Phe	sec	$10.21^{+0.2}_{-0.21}$	0.84	$83.04^{+1.63}_{-0.83}$	$77.5^{+1.4}_{-1.1}$
V1276 Sgr	sec	$87.7^{+1.2}_{-9.1}$	0.81	$143.8^{+4.9}_{-7.2}$	$289.1^{+1.4}_{-5.7}$
BW Vel	sec	$73.6^{+2.2}_{-20.2}$	0.94	$66.3^{+16.8}_{-7.4}$	$209.64^{+0.69}_{-7.02}$
OQ Vel	prim	$12.0^{+5.0}_{-2.2}$	0.77	$70.3^{+37.5}_{-6.5}$	$130.1^{+14.5}_{-4.4}$
MW Vir	prim	$10.77^{+0.35}_{-0.46}$	0.78	$137.32^{+0.78}_{-1.53}$	$94.22^{+2.96}_{-0.83}$

Results: LCs fits and models

DN UMa P = 1.730 d

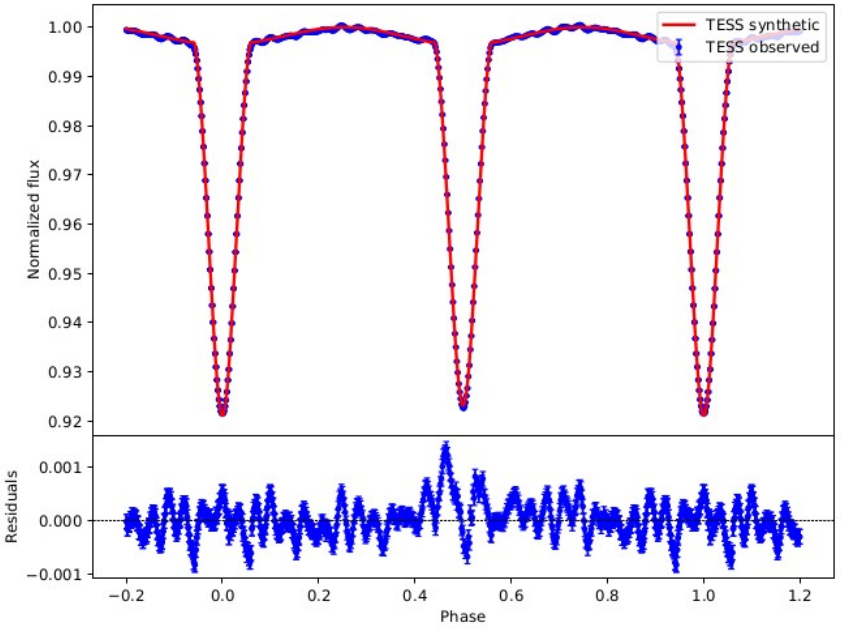

V0884 Mon P = 0.356 d

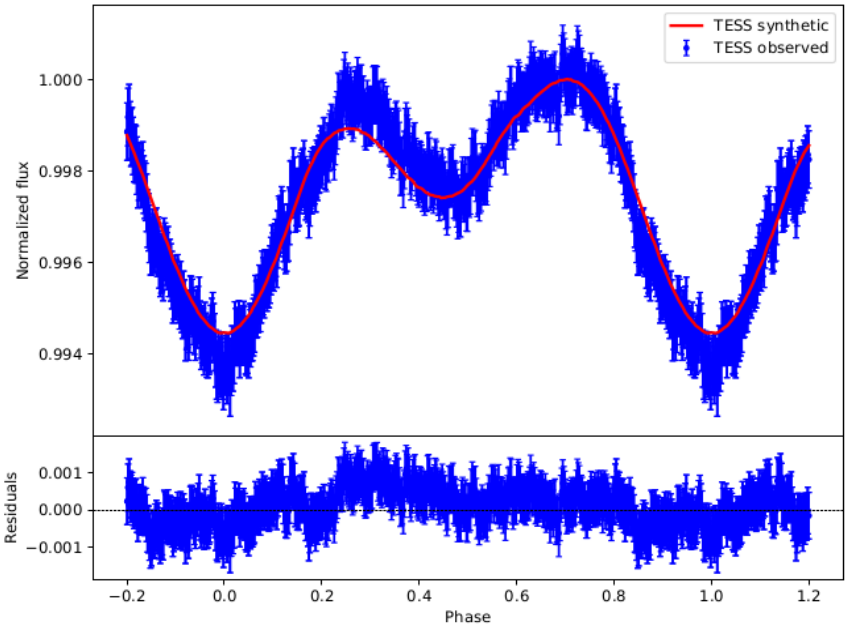

Results: LCs fits and models

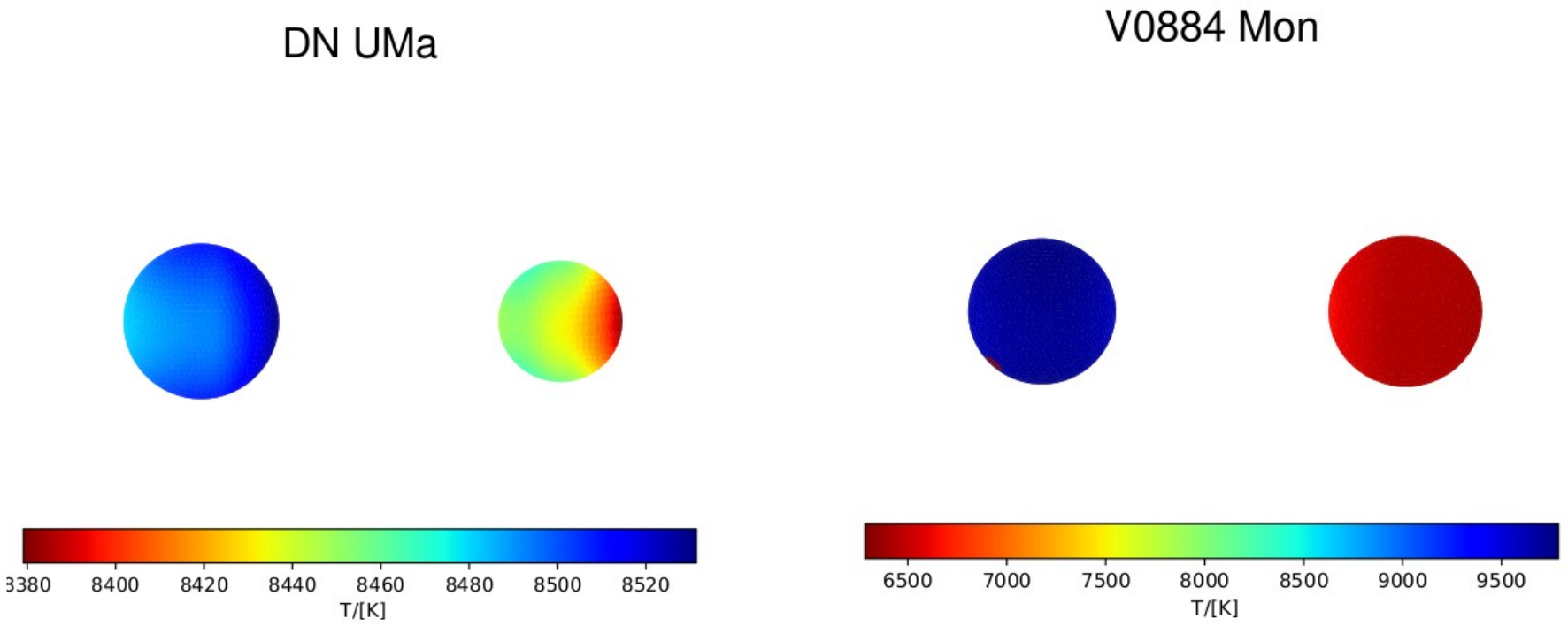

Results: LCs fits and models

BH Nor

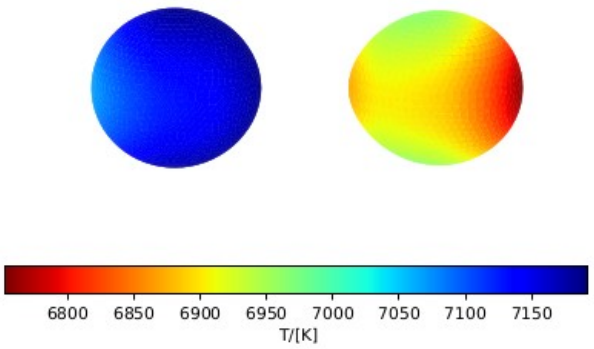

GX Nor

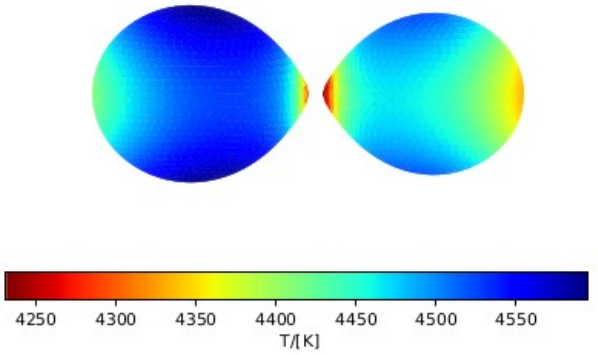

OT Nor

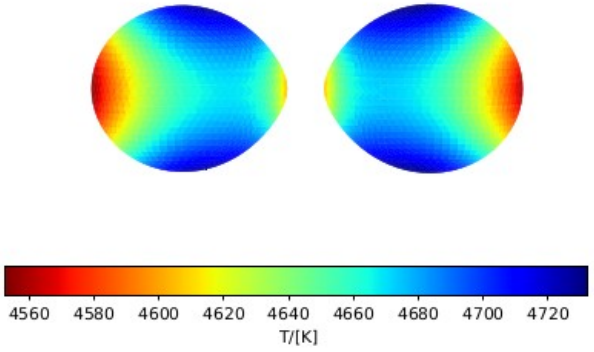

KR Per

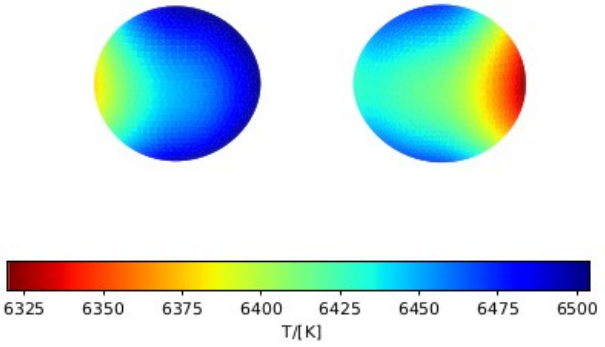

Results: Orbital Period vs. (J-K)

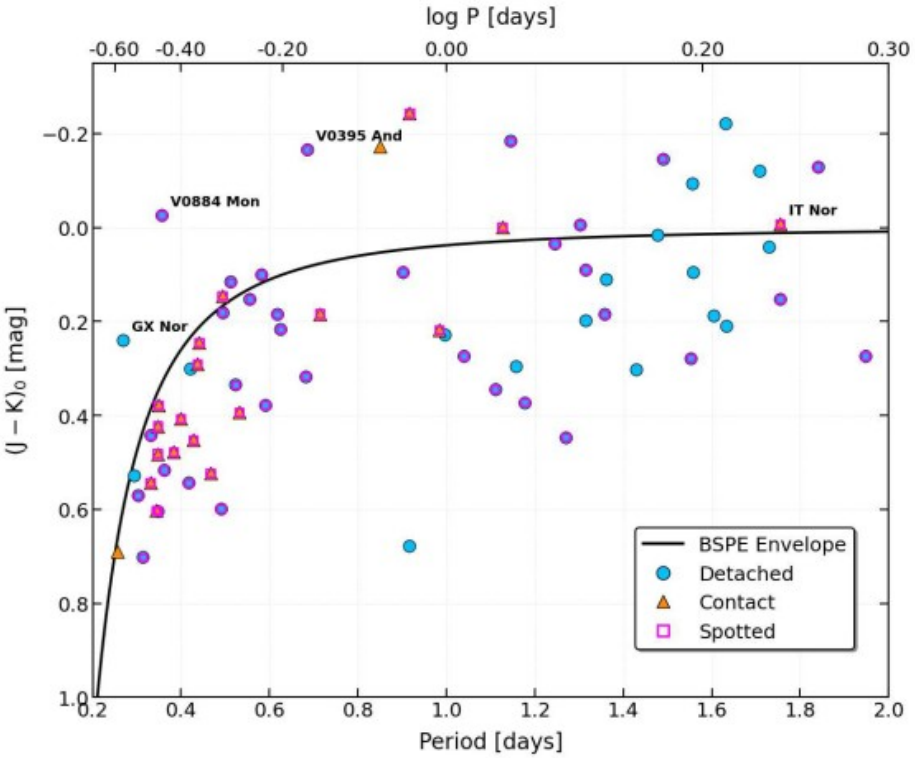

- The Period–Color distribution - a different behaviour for detached and contact binaries
- Contact binaries - main-sequence objects, are confined to a narrow sequence defined by the Blue Short-Period Envelope (BSPE).
- Systems bluer than the BSPE for a given period very probably host a hot third component affecting the observed color. Systems which are too red for a given color can also be affected by interstellar extinction.
- Detached binary stars can contain components at different evolutionary stages affecting their observed color.

Results: Temperature vs. (J-K)

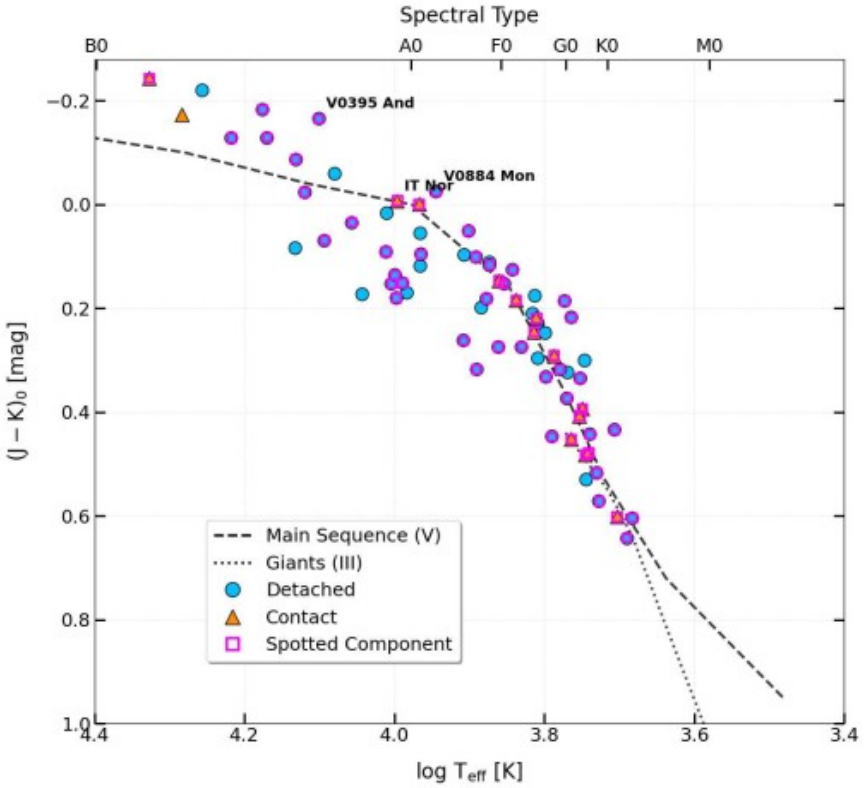

- Most systems follow the expected MS trend, with detached binaries exhibiting a broader distribution, including a shift toward redder (cooler) colors.
- In contrast, contact systems are more tightly clustered along the main-sequence locus, consistent with their thermally coupled envelopes.
- The agreement with the theoretical dwarf sequence and partial overlap with the giant track for cooler systems suggests a mix of evolutionary stages within the sample, particularly among detached binaries

Results: EBs with atypical positions in our sample

- *IT Nor*: P = 1.7541 day, is unusually long for, CBs which generally have $P < 1$ day (Rucinski 1998; Rucinski & Pribulla 2008).
- With the relatively large q = 0.74, this suggests that a classical contact config. is unlikely.
- Semi-detached or near-contact eclipsing binary, possibly of Algol type, in which one component fills or nearly fills its Roche lobe while the other remains detached.
- Such systems commonly exhibit orbital periods in the range of 1–3 days and often contain early-type primaries.
- Representation of a transitional system evolving toward contact through mass transfer and angular-momentum redistribution (e.g., Paczyński 1971, Eggleton 2006).

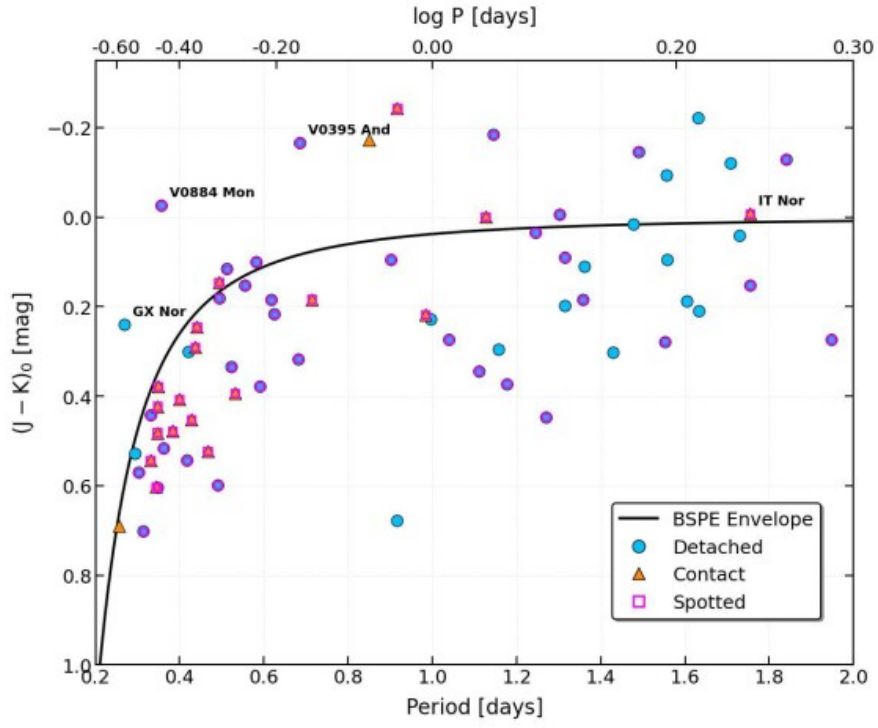

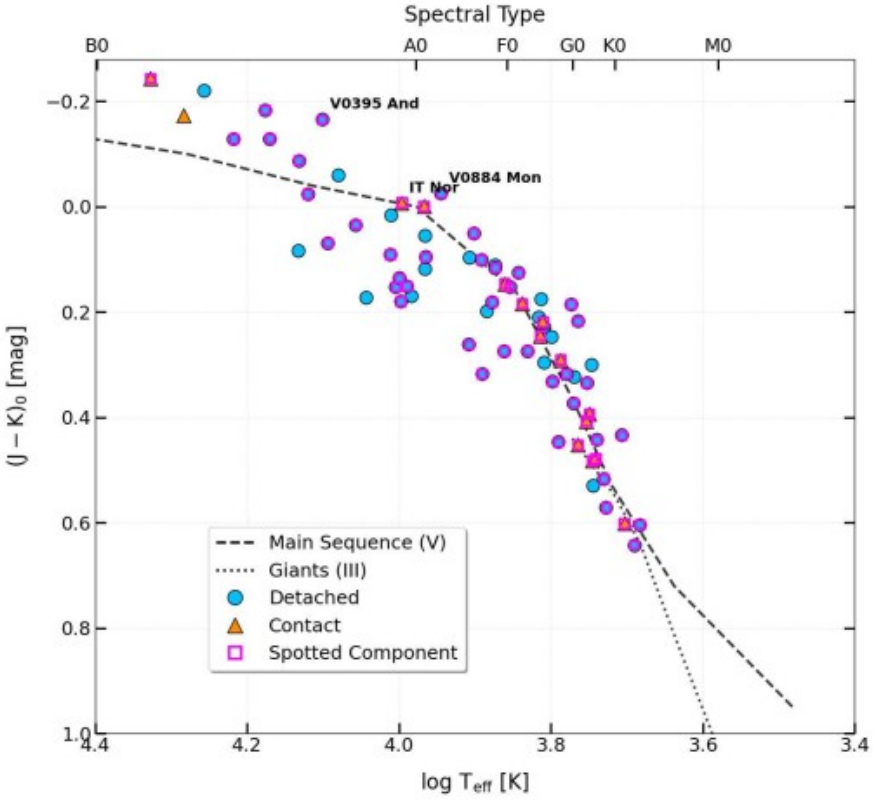

Results: EBs with atypical positions in our sample

- *GX Nor:* P = 0.2688 day, unusually short for a detached system.
- Detached eclipsing binaries are typically found at periods longer than ~ 1 day, while systems with $P < 0.3$-0.4 day are overwhelmingly associated with contact (W UMa-type) configurations (Rucinski 1998; Norton et al. 2011).
- If *GX Nor* is genuinely detached, both components must be compact, low-mass stars well within their Roche lobes. However, at such short separations, tidal interactions are strong and are expected to drive the system toward contact on relatively short evolutionary timescales
- *GX Nor* is most plausibly interpreted as either a rare short-period detached binary composed of low-mass stars or, more likely, a near-contact system on the verge of Roche lobe filling.

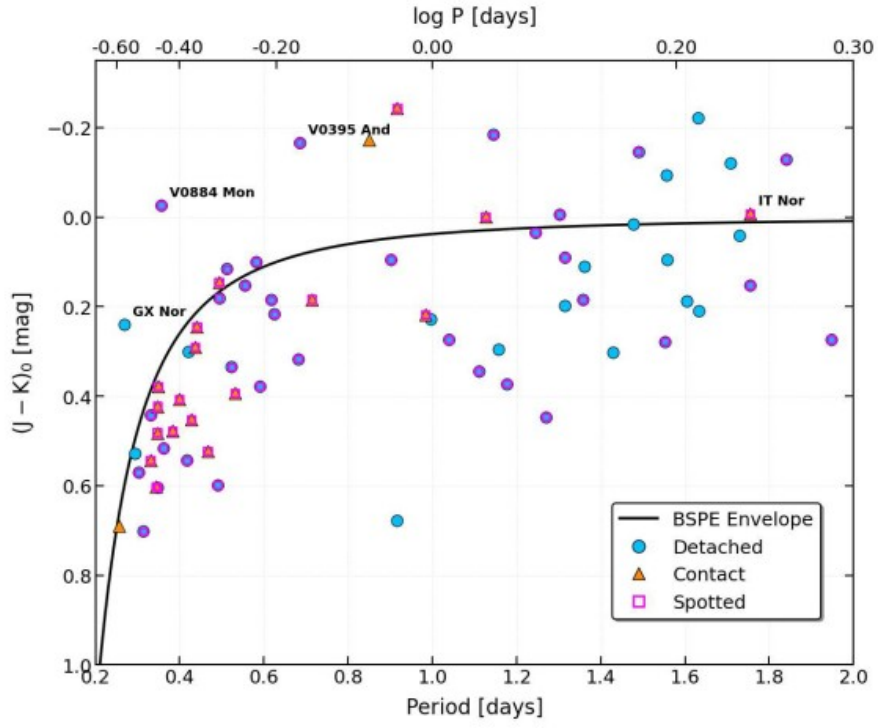

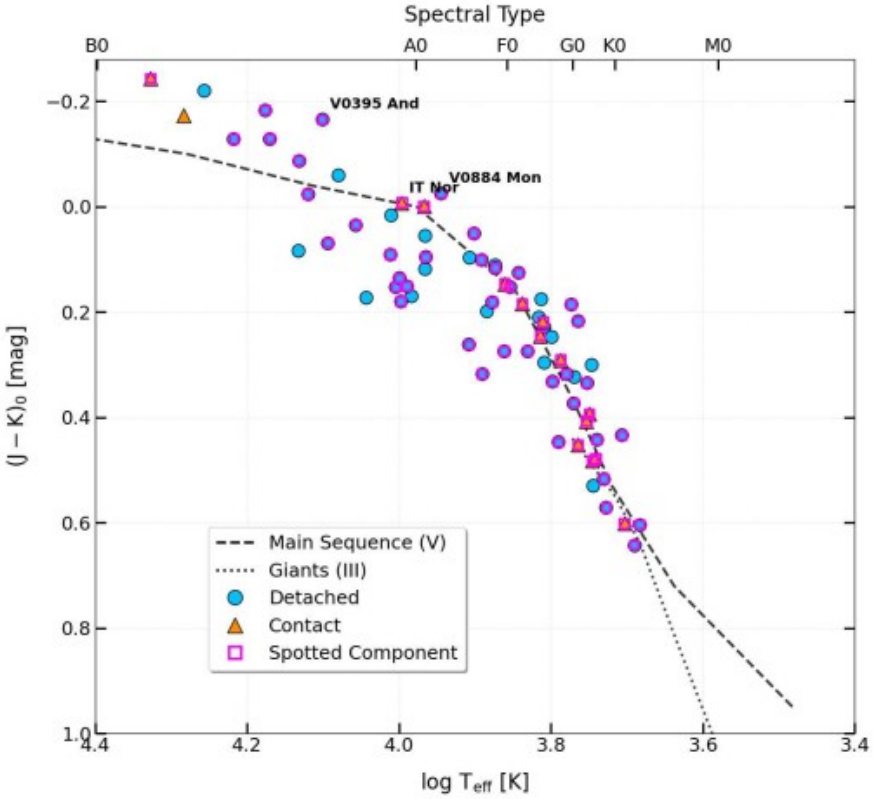

Results: EBs with atypical positions in our sample

- *V884 Mon:* P = 0.3559 day, a near-infrared ($J - K$) = -0.026, q = 0.94, and $i \approx 59$ degr.

- The negative color index - relatively hot system early-type (A–B) comp. (Bessell & Brett 1988) - unusual for such short-period binaries that are typically composed of cooler, late-type stars.

- For early-type stars, which have relatively large radii, such a short period implies a very small orbital separation, making a detached configuration difficult to maintain.

- q = 0.94 suggests nearly equal-mass components, a property rather unusual for contact binaries. In addition, $i \approx 59$ degr. implies partial eclipses, which can introduce degeneracies in the photometric solution and increase uncertainties in the derived parameters.

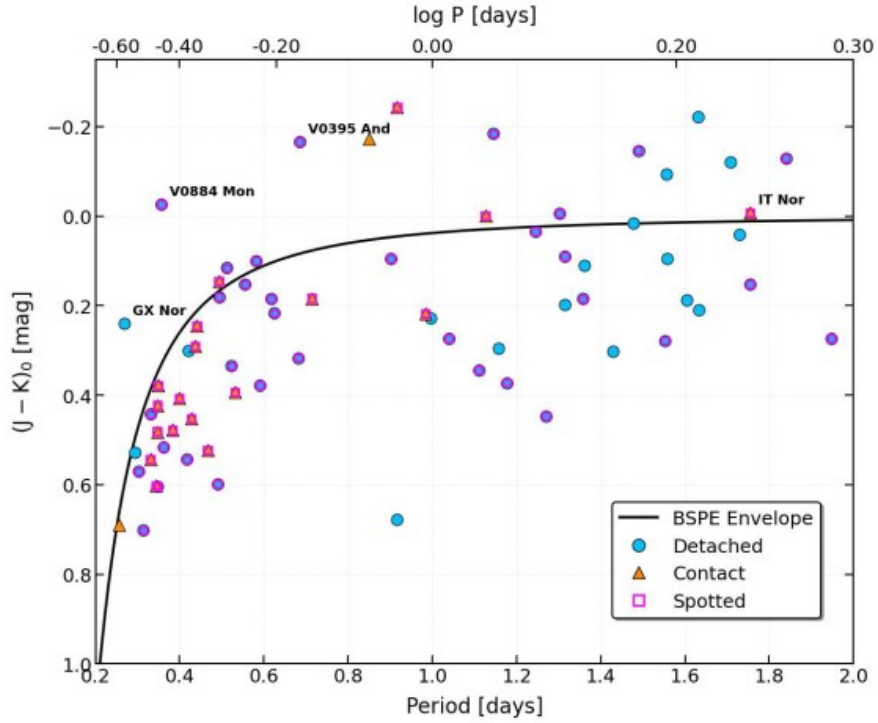

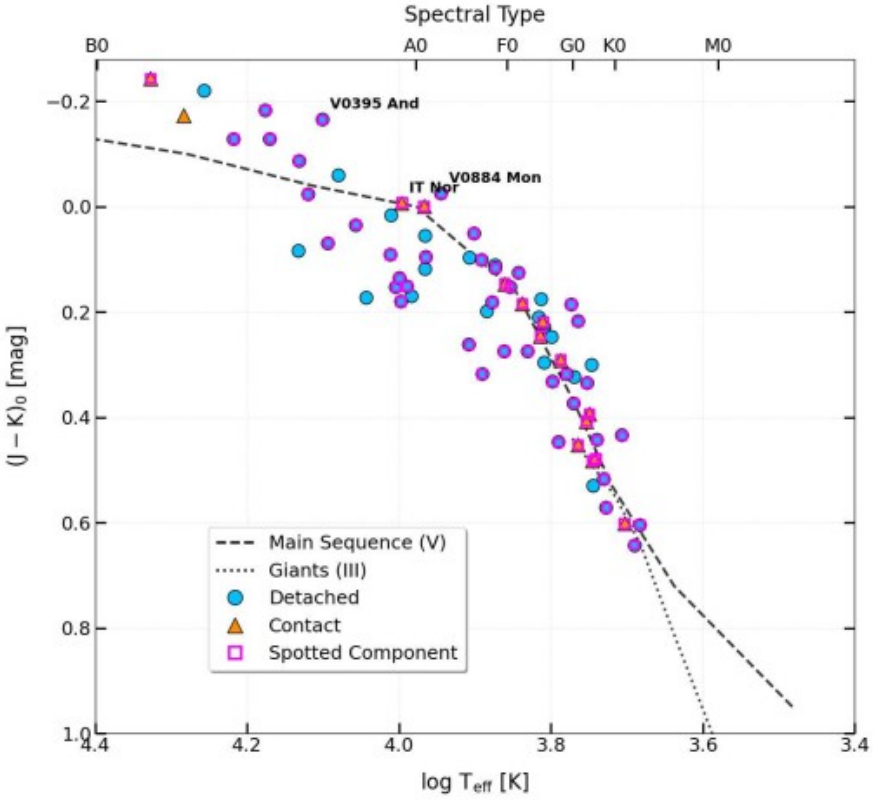

Results: EBs with atypical positions in our sample

- *V395 And:* P = 0.6847 day, $T_{\rm eff}$ ≈ 12600 K, a near-infrared color index ($J - K$) = -0.116, q = 0.762, and inclination i ≈ 56 degr. (late B–early A).

- Atypical for short-period binaries that are usually composed of cooler, late-type stars.

- *Rucinski (2005):* spectroscopic mass-ratio (0.879±0.025) in contrast with photometric one (0.762±0.048).

- The combination of high temperature, short period, and relatively high mass ratio suggests that the system lies near the boundary between detached and contact configurations.

- It is possible that V395 And is a near-contact or shallow-contact system, rather than a classical detached binary.

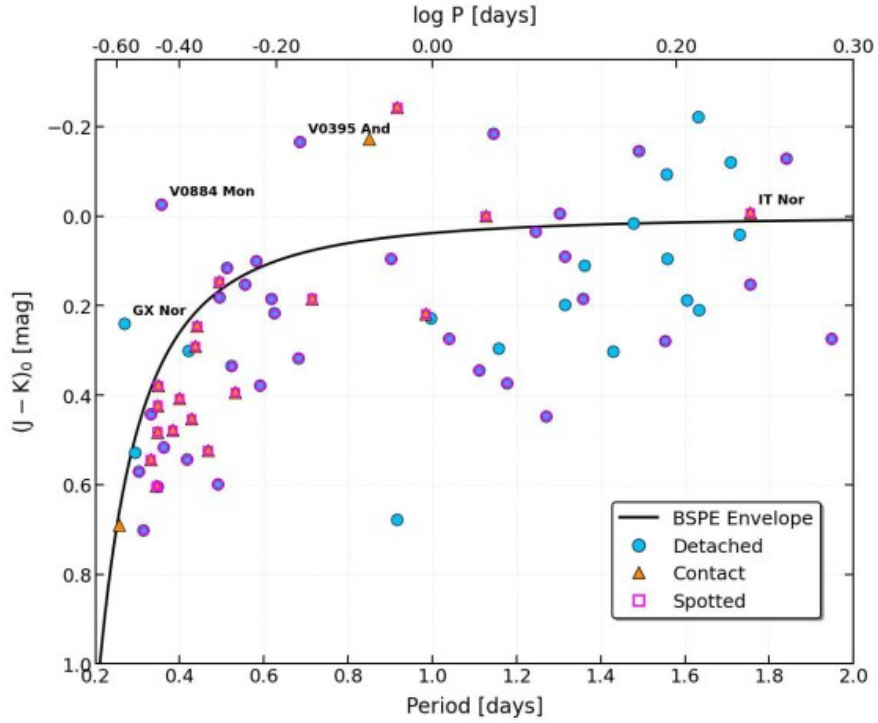

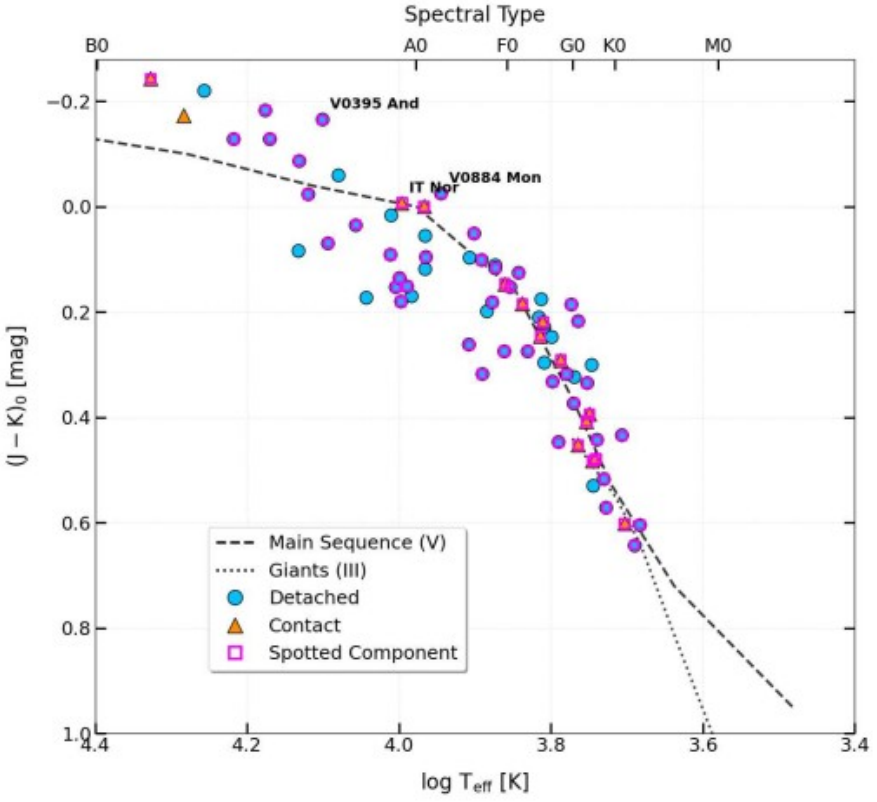

Results: Single-parameter distribution

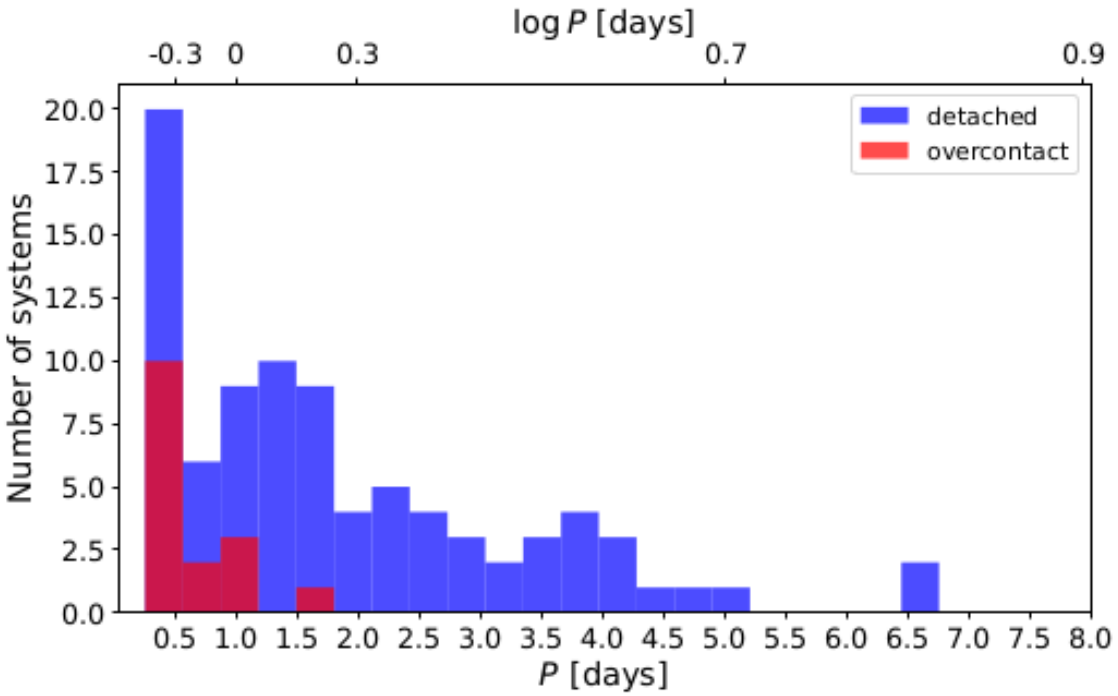

- Concentration of DBs and CBs at short periods, with a dominant peak between $P \simeq 0.29$ and 0.5 days - typical for contact binaries.
- For DBs the peak near 0.29–0.5 days generally indicates a population of very close, tidally evolved binaries that are likely approaching the contact stage or are dynamically linked to contact-binary evolution.
- DBs additionally show a secondary peak between 1 and 1.8 days, while the remaining binaries are distributed across 1.8 - 5 days.
- Similar period distributions - large eclipsing-binary surveys (Prša et al. 2011)

Results: Single-parameter distribution

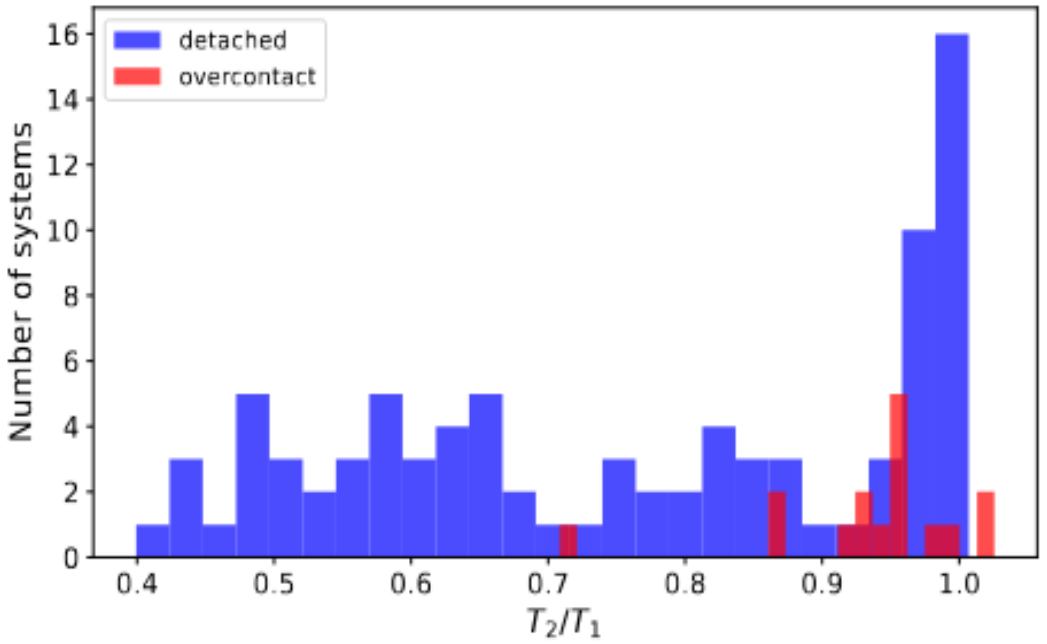

- Detached systems strongly cluster near $T_2/T_1 \simeq 0.95 - 1.0$ - binaries contain components with similar effective temperatures and evolutionary states.
- Expected for detached (MS) binaries with comparable M_1,M_2; and these systems are also more easily detected because they produce eclipses of similar depth.
- Detached binaries, distributed over $T_2/T_1 \simeq 0.4 - 0.9$, likely reflect a broader range of stellar masses and evolutionary stages, since detached components evolve largely independently prior to mass transfer.

Results: Single-parameter distribution

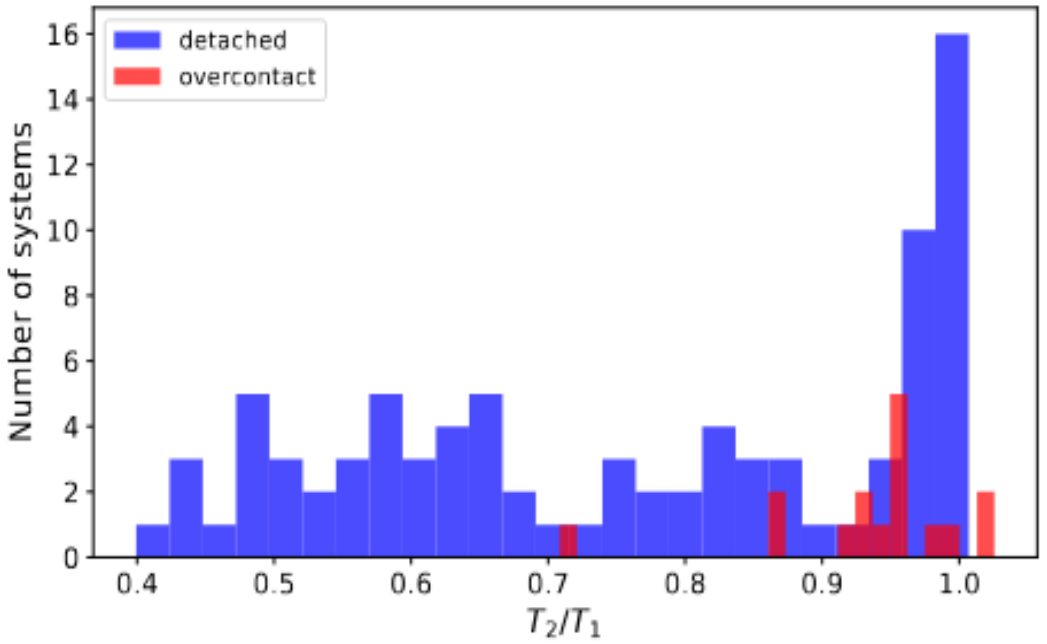

- The contact systems show a strong peak near $T_2/T_1 \simeq 0.95$, consistent with thermal coupling through a common convective envelope.
- In contact binaries, energy transfer between the components tends to reduce temperature differences and drive the system toward thermal equilibrium (Lucy 1968)
- Contact systems with $T_2/T_1 > 1$ may correspond to W-subtype systems, in which the less massive component appears slightly hotter because of magnetic activity, starspots, or energy-transfer effects within the common envelope (Binnendijk 1970).

Results: Single-parameter distribution

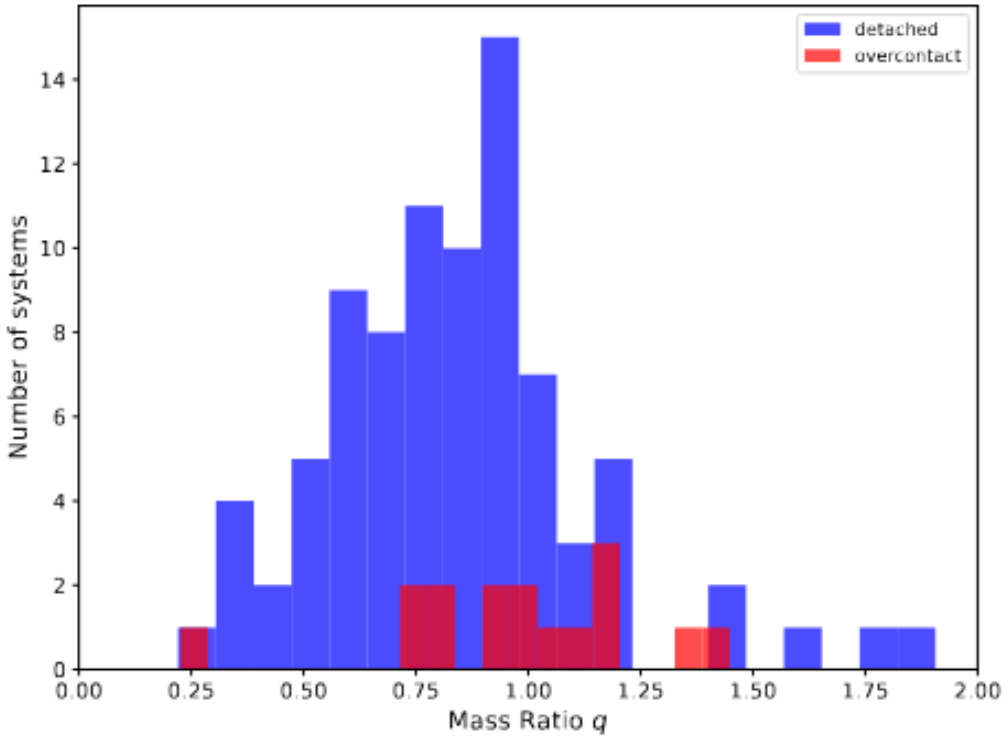

- The observed q (M_2/M_1) distribution of our sample appears broadly consistent with the expected evolutionary separation between detached and contact configurations.
- DBs are preferentially detected when the stellar components have comparable radii and luminosities, conditions that are commonly associated with nearly equal masses.
- The presence of detached and contact systems with $q > 1$ ($1.25 \lesssim q \lesssim 1.85$) likely indicates binaries that have undergone significant mass exchange.
- Roche-lobe overflow can reverse the original mass hierarchy, leaving the initially less massive star as the present-day accretor and the more massive component as the donor.

Results: Asymmetric Uncertainties in Photometric Solutions

- The photometric solution presented here shows that the uncertainties of key photometric elements (q, i, T, Ω) are frequently asymmetric, and sometimes markedly so.
- Reflects the intrinsic structure of the inverse problem and the limitations of photometric modeling (Wilson & Devinney 1971; Prša & Zwitter 2005).
- The photometric elements are often strongly correlated, allowing different parameter combinations to produce similarly acceptable fits.
- As a result, the χ^2 surface becomes skewed, yielding unequal upper and lower confidence intervals.

Results: Asymmetric Uncertainties in Photometric Solutions

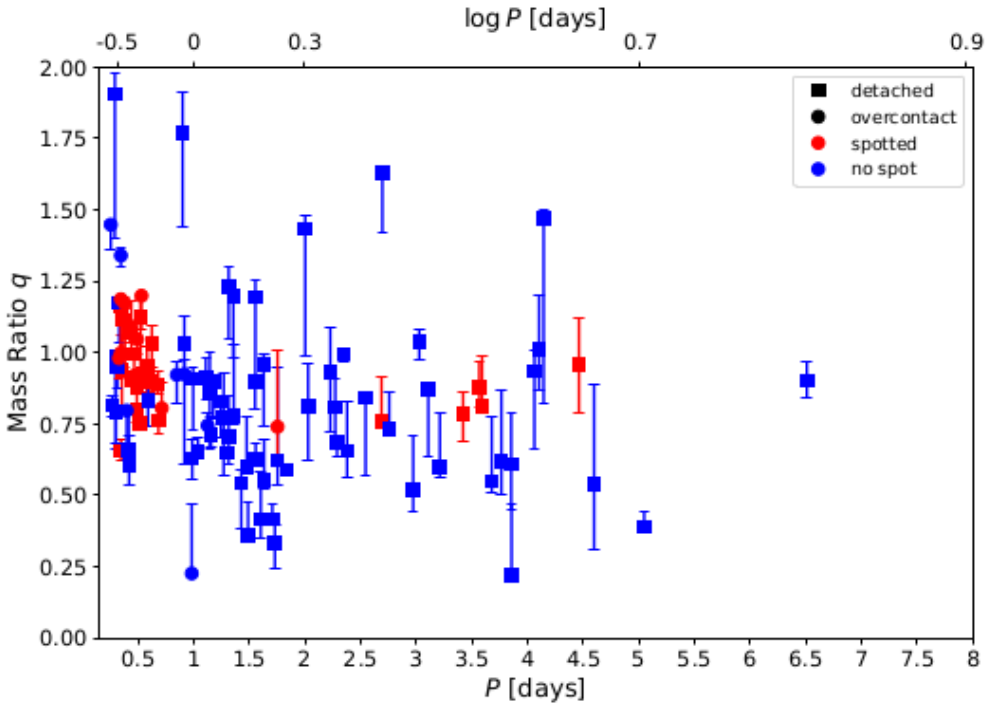

- The photometric solution presented here shows (q, i, T, Ω) are frequently asymmetric, and some
- Reflects the intrinsic structure of the inverse pro (Wilson & Devinney 1971; Prša & Zwitter 200
- The photometric elements are often strongly co to produce similarly acceptable fits.
- As a result, the χ^2 surface becomes skewed, yiel
- The asymmetric errors often reported in photometric solutions of eclipsing binaries (as in our study) arise from:
  - a combination of nonlinear model behaviour,
  - strong parameter degeneracies,
  - incomplete observational constraints,
  - additional model complexity,
  - boundary effects, and the use of modern statistical methods.

Future work

- The results of this study suggest avenues for further research into the presented sample of objects, with the potential to explore and investigate them in more detail.
- In the future, we intend to examine residuals from light-curve fits to identify additional changes that could shed further light on their physical nature.
- Furthermore, we intend to analyse the (LCs) of all 14 objects with peculiar shapes, which are listed in the supplementary material of this work.
- The presented sample also provides interesting candidates for spectroscopic follow-up, with brightnesses up to V = 12–13 mag.

Future work

- The results of this study suggest avenues for further research into the presented sample of objects, with the potential to explore and investigate them in more detail.
- In the future, we intend to examine residuals from light-curve fits to identify additional changes that could shed further light on their physical nature.
- Furthermore, we intend to analyse the (LCs) of all 14 objects with peculiar shapes, which are listed in the supplementary material of this work.
- The presented sample also provides interesting candidates for spectroscopic follow-up, with brightnesses up to V = 12–13 mag.

Thank you for your listening